CHANGE OF PLASMA PROPERTIES PRIOR TO HIGH DENSITY DISRUPTIONS IN ASDEX

H. Niedermeyer, K. Behringer, K. Bernhardi, A. Eberhagen, G. Fussmann, O. Gehre, J. Gernhardt, G. Haas, M. Keilhacker, S. Kissel[+], M. Kornherr, G. Lisitano, J. Massig, K. McCormick, D. Meisel, E.R. Müller, H. Murmann, J. Neuhauser, W. Poschenrieder, B. Richter, G. Siller, F. Söldner, K.-H. Steuer, Z. Szymanski[++]

IPP III/90 October 1983

MAX-PLANCK-INSTITUT FÜR PLASMAPHYSIK

8046 GARCHING BEI MÜNCHEN

MAX-PLANCK-INSTITUT FÜR PLASMAPHYSIK

GARCHING BEI MÜNCHEN

CHANGE OF PLASMA PROPERTIES PRIOR TO HIGH DENSITY DISRUPTIONS IN ASDEX

H. Niedermeyer, K. Behringer, K. Bernhardi, A. Eberhagen, G. Fussmann, O. Gehre, J. Gernhardt, G. Haas, M. Keilhacker, S. Kissel[+], M. Kornherr, G. Lisitano, J. Massig, K. McCormick, D. Meisel, E.R. Müller, H. Murmann, J. Neuhauser, W. Poschenrieder, B. Richter, G. Siller, F. Söldner, K.-H. Steuer, Z. Szymanski[++]

IPP III/90 October 1983

[+] On leave from Massachusetts Institute of Technology, Cambridge, USA

[++] On leave from Institute of Fundamental Technological Research, Warsaw, Poland

Die nachstehende Arbeit wurde im Rahmen des Vertrages zwischen dem Max-Planck-Institut für Plasmaphysik und der Europäischen Atomgemeinschaft über die Zusammenarbeit auf dem Gebiete der Plasmaphysik durchgeführt.

IPP III/90 H. Niedermeyer, et al.

CHANGE OF PLASMA PROPERTIES PRIOR TO HIGH DENSITY DISRUPTIONS IN ASDEX

October 1983

ABSTRACT

An anomalous state of the plasma boundary has been found in divertor and limiter discharges near the density limit in the ASDEX tokamak. The plasma parameters are no longer constant on flux surfaces near the boundary. A toroidally symmetric belt shaped region with densities above the central value and very low temperatures develops at the inner side of the torus. Strongly enhanced radiation from impurity ions in low ionization states is emitted from this plasma region while the mean impurity concentration of the discharge remains unchanged.

The drastic change of the parameters in the plasma boundary might be explained by a thermal instability which can appear if the parallel heat conduction time is longer than the local cooling time. This implies that the transverse energy flow from the central plasma to the inner boundary is small. This limitation of heating power in the plasma boundary might be the cause of the density limit of tokamaks.

I. INTRODUCTION

In the ASDEX divertor expriment, as in all major tokamaks, any increase of the plasma density during a discharge by means of programmed or feedback-controlled gas puffing is limited by a disruptive instability. The disruption is preceded by a strongly growing MHD mode. In a wide parameter range, however, the first indications of the density limit being reached are observed a few tens of milliseconds before the MHD instability appears: the line-averaged electron density increases faster than programmed via a fast gas valve, the loop voltage increases, the intensity of H_α increases by a factor of 2, the bolometer signals increase by a factor of 2 or 3, and the intensity of CIII and OIII lines increases by about two orders of magnitude (Fig. 1a and 2). By skillful programming of the density increase it was possible to sustain this predisruptive plasma state for about 600 ms while n_e was steadily growing even above the normal density limit (Fig. 1b, 3, 4a).

In discharges with a "mushroom" limiter on the outer periphery of the torus a similar state automatically develops at density plateaus slightly below the limit (Fig. 4b). As shown in the following, the pre-disruptive (p.d.) state is characterized by a strong poloidal asymmetry of plasma parameters near the boundary, namely a belt-shaped strongly radiating high-density region near the inner periphery of the torus. This region is probably identical to the "marfes" observed in ALCATOR C /1/. In ASDEX the phenomenon was mainly investigated because there is a strong suspicion that when this state becomes unstable it triggers MHD instabilities and thus determines the density limit. Moreover, it may be of interest with respect to a radiating plasma mantle and also for basic transport studies.

II. EXPERIMENTAL FINDINGS

2.1 Temperature and Density Profiles, Electromagnetic Parameters

The electron temperature and density profiles of the hot plasma core ($r < 0.3$ m = 0.75 a) in a divertor discharge (H_2, I_p = 250 kA, B_o = 2.17 T,

$q_a = 4.3$) are measured by ECE-radiometry and Thomson scattering. During the p.d. state a slight reduction of the temperature in the core and a peaking of the T_e-profile is observed. The profiles before and during the p.d. state are approximated by the following analytical form:

$$T_e = 550 \cdot \exp(-20\, r^2 - 12.3\, r^4)$$
$$\rightarrow 500 \cdot \exp(-18.5\, r^2 - 84.4\, r^4)$$

$$n_e = 4.5 \cdot 10^{19} (1 - 5.13\, r^2 + 4.68\, r^4 - 14.9\, r^6)$$
$$\rightarrow 5.6 \cdot 10^{19} (1 - 5.13\, r^2 + 4.68\, r^4 - 14.9\, r^6)$$

where T_e is in eV, r in m and n_e in m^{-3}. The first expression is valid for the normal state immediately before the transition, the second one for the p.d. state immediately after the transition. For the ion temperature profile the same shape is assumed, but a slightly lower central value ($T_{io} = 530$ eV $\rightarrow$ 480 eV). Z_{eff} is essentially 1. Assuming Spitzer's conductivity without any corrections, one calculates $q_o = 0.89 \rightarrow 0.81$, $l_i = 1.49 \rightarrow 1.66$, $\beta_p = 0.30 \rightarrow 0.31$, $U_L = 1.42$ V $\rightarrow$ 1.77 V. All these approximative values agree well with spectroscopic and electromagnetic measurements. The values of $q_o < 1$ are in agreement with the observation of sawtooth activity. The discharge boundary is feedback-centred in the radial direction within 3 mm, and in the vertical direction within much less than 1 mm; the plasma current is kept constant within 1 kA.

While the plasma core during the p.d. state only shows a slight reduction of temperature and peaking of profiles, drastic changes of the density profile in the plasma boundary must be concluded from interferometric measurements. Seven equidistant horizontal 2 mm microwave channels, 3 horizontal HCN channels at $z = 0$ and $\pm a/2$ and one vertical channel through the plasma centre are available in ASDEX. Profile measurements with the 2 mm interferometer are possible until the transition; during the p.d. state the measurement is strongly perturbed. The vertical and horizontal centre channels of the HCN interferometer agree well in the normal state (a correction for the divertor plasma which is also seen by the vertical channel has to be made in divertor discharges).

During the p.d. state the two channels differ by typically 6 % to 10 % (Fig.4a). From this a poloidally asymmetric density hump off-axis must be concluded. We strongly suspect that the region of intense impurity line radiation at the inner periphery of the torus observed in photographs

(Fig. 8) is the region of anomalously high density. (Because of pressure equilibrium on flux surfaces it must also be a region of anomalously low temperature.) No direct measurement of density or temperature is available for this region. The following arguments should therefore support the identification of the strongly radiating plasma zone with the density hump.

At the outer periphery density profiles of the plasma edge are measured with high time resolution by means of a neutral lithium beam (Fig. 5). One observes a slight flattening of the density profiles outside the separatrix at the transition to the p.d. state (1/e length = 5 cm → 7.6 cm), the density at the separtrix staying constant. Within error bars the boundary-Thomson scattering system gives the same result.

All the horizontal HCN interferometer channels show strong fluctuations (Fig. 4a and 6) during the p.d. state (the peak - to - peak amplitude is typically 3 % of the mean value). The fluctuations on the two channels at a/2 above and below the midplane are strongly correlated with 180^{o} phase difference. This is explained by the assumption that the wings of the density hump reach /z/= a/2, and that the hump's position fluctuates in the vertical direction.

A slight vertical shift of the plasma centre ($\pm$ 2 mm) causes an equidirectional shift of the bright zone observed in pictures, increased by a factor of about 100. The asymmetry observed in this case on the HCN channels at $z = \pm a/2$ again confirms the identity of the strongly radiating and dense plasma zones.

During discharges with a mushroom limiter in the midplane at the outer periphery the general behaviour of the signals discussed up to now is the same. As Z_{eff} is >1, temperatures are higher (T_{eo} = 1060 eV → 970 eV) and the density limit is only about half the value of that in divertor discharges. The density hump in stationary phases of the p.d. state in limiter discharges is well centred in vertical directions; a top-bottom asymmetry is observed during the density rise and decay at the beginning and end of the p.d. state (Fig. 4b) . From an excess of the horizontal density integral of 6 % and an assumed width of the density hump of 5cm (which is about 6 % of the plasma diameter and is based on the width of the bright zone of the CII line) one calculates a peak density of the hump as high as the density on the plasma axis, i.e. $5.6 \times 10^{19}\ m^{-3}$, which is more than 3 times the

value of 1.75×10^{19} m^{-3} extrapolated from the plasma core profile and 7 times higher than the value of 8×10^{18} m^{-3} measured by laser light scattering in the outer boundary.

The evaluation of T_e profiles at the plasma edge from the Thomson scattering system are problematic since the signals from the three spectral filters applied can hardly be fitted with a Gaussian. If one omits the high-energy channel, a temperature decrease in the plasma boundary during the p.d. state is observed and one calculates temperature profiles compatible with all other measurements and assumptions: the T_e is low enough to allow stationary temperature gradients along the magnetic field lines at reasonable power fluxes, and the surfaces of constant T_e shrink towards the plasma centre in agreement with spectroscopic observations. The overthermal high-energy component observed is, however, of physical interest and must be further investigated.

2.2 Fluctuations, Modes, Disruption

Fluctuations on the HCN channels at $z = \pm a/2$ were mentioned in the previous section. Signals from soft-X-ray diodes, the observation chords of which have a similar distance from the plasma centre, show fluctuations strongly correlated with the interferometer signals (Fig. 7). (The upper diode signal fluctuates in phase with the upper interferometer signal.) As both diagnostics are at a toroidal distance of 180°, a strong correlation of the high-density belt in the toroidal direction must be concluded. The fluctuations are random and not correlated with sawtooth activity.

No correlation has yet been found between the fluctuations on the horizontal centre HCN channel, the horizontal centre soft-X-ray channel, the Li beam signals and any other HCN channels or soft-X-ray channels.

The transition to the p.d. state has no influence on any stationary mode activity. This again indicates that the p.d. state is only a boundary phenomenon. At too high densities a rapdily growing MHD mode with a frequency of about 5 kHz leads to a minor disruptive instability. Depending on the discharge conditions, this happens a few tens of milliseconds after the transition to the p.d. state or a few hundred milliseconds after the

transition at the end of a slow density rise in divertor discharges. If the gas valve is closed in time, a transition to the normal state without disruption occurs.

2.3 Spectroscopic, Photographic and Bolometric Measurements

Photographs of the discharge were taken in the tangential direction through different narrow band interference filters centered at H_α, H_β and strong impurity lines in the visible: OII (4416 Å), CII (5133 Å), CrI (5393 Å). Examples of the emission before and during the p.d. state are shown in Fig. 8a - f.

As expected, all lines mentioned are emitted only from the plasma boundary. During the normal plasma state of divertor discharges the hydrogen and impurity lines are excited mainly in the divertor throats and from the plasma boundary regions next to the divertor entrance. Because hydrogen and impurities mainly recycle at the divertor plates, the divertor is the main source of neutral hydrogen and of impurities in low ionization states. The majority of H^o, CII and OII particles do not reach the boundary regions next to the midplane.

Pictures from the p.d. state are quite different: hydrogen is still excited in the divertor throats, but there is scarcely any impurity line emission in the divertor throats. The reduced temperature of the divertor plasma (measured with Langmuir probes) during the p.d. state is no longer sufficient to excite the CII or OII lines (E = 23.1 eV/26.2 eV), but still H_α and H_β (E = 12.0 eV/12.7 eV). A slight reduction of impurity recycling through the divertor cannot be ruled out (the partial pressure of H_2O stays constant, that of CO drops slightly during the p.d. state, while the H_2 pressure increases) but cannot explain the lack of impurity light quantitatively.

More astonishing is the strong emission of impurity lines and the enhanced emission of hydrogen lines at the inner plasma boundary with peaking near the midplane. The zone of strong radiation has a lens-like cross-section about 5 cm wide and 30 cm high.

The spatial distribution of impurity line radiation was quantitatively investigated by radial scans with VUV spectrometers the tilting axis of which is in the midplane. Figures 9 and 10 show a comparison of measured profiles from different ionization states of carbon and oxygen. All impurity lines measured are strongly enhanced during the p.d. state, the enhancement factor being the lower the higher the ionization level (OIV: 12, OV: 6, OVI: 3, CIII: ≈ 30, CIV: ≈ 1.5).

All lines but the lowest (OII, CII) show the structure of nearly homogeneous thin toroidal shells with a radius equal to or slightly smaller than the plasma radius. This indicates that the density of the specific impurity ions and the plasma parameters are constant on flux surfaces near the boundary.

During the p.d. state the emission of the higher ionization states (OIV, OV, OVI) stays homogeneous in the poloidal direction, but the radius of the radiating shell shrinks by about 5 cm (see OVI profile from limiter discharge). This is consistent with a shrinking of the T_e profile which can also be concluded from the broader H_α layer observed in photographs. Changes of the T_e profile can at least partly explain the increase of intensity since the excitation energy of these lines is much smaller than the ionization energy of the specific ions.

The explanation of the peaked profiles from the lower states is not straight forward. Some essential arguments are collected in the section "Summary and Discussion".

At this point the simplest argument for the increase of impurity emission - enhanced plasma wall contact - must be excluded. An evaluation of absolutely measured intensity profiles of higher ionization states (OVIII: λ = 19.0 Å, Fe XVII: λ = 15.01 Å) shows that the impurity concentration on axis stays essentially constant (oxygen: $7.5 \times 10^{-4} \rightarrow 9.8 \times 10^{-4}$, iron: $8.4 \times 10^{-6} \rightarrow 9.1 \times 10^{-6}$ in divertor discharges). A strongly increased influx would have to be compensated by exactly the same decrease in impurity confinement. This hypothetic influx of particles should finally be swept into the divertor and should there cause a higher pressure of H_2O and CO, which is not

observed. Finally, there is no evidence of enhanced plasma-wall interaction in photographs - taken either in the tangential or in the radial direction directly showing protruding parts of the inner vessel structure.

Figure 11 shows the time history of different impurity lines at the transition.

The total radiation profile of a divertor discharges was taken with a radially scanning bolometer (Fig.12) with the tilting axis in the midplane, similar to the spectroscopic scans. During the normal state the profile is that of a thin, homogeneously radiating shell as is generally observed in discharges contaminated mainly by light impurities. During the p.d. state a contribution of radiation from the near-midplane region is observed (a contribution from the hot plasma centre can be excluded since the heavy impurity concentration stays low and T_{eo} is lower in the p.d. state than before). The total radiation level increases from 47 kW to 129 kW, i.e. with a change in ohmic power from 348 kW to 434 kW radiation losses from the plasma torus increase from 14 % to 30 %.

With a spectrometer calibrated at Ly-ß the absolute intensity of a few lines can be determined or at least estimated. In the p.d. state the 1032 Å OVI line emits about 20 kW, Ly-α radiates about the same power. The sum of OII and OIII lines at 834 Å gives about the same signal amplitude as the 1032 Å OVI line, i.e. the power emitted by the lower ionization states of oxygen is of the same order of magnitude as the OVI radiation. The radiation from the high density zone at the inner plasma boundary significantly contributes to the energy balance of the discharge.

III. SUMMARY AND DISCUSSION

As shown in the previous sections, at very high densities slightly below the density limit in ASDEX a pre-disruptive plasma state develops. It is characterized by strong poloidal asymmetries in the plasma boundary zone. At the inner periphery there exists a belt-shaped zone with lense-like

cross-section and strong toroidal coupling in which the electron density is much higher and the temperature is much lower than outside. This zone emits strong impurity radiation especially of the lowest ionization states; hydrogen radiation from this zone is slightly increased. The phenomenon is independent of divertor or limiter operation of ASDEX.

The pre-disruptive state is most probably the result of a thermal poloidal instability on closed flux surfaces near the plasma edge. An oversimplified model may show the principle of the mechanism. We assume the radiated power density p_r to depend on the electron density n_e, the impurity ion density n_I and the electron temperature T_e according to

$$p_r \sim n_e \cdot n_I \cdot T_e^{\nu},$$

where ν is a constant coefficient. At low T_e and high n_e there is a strong collisional coupling between impurities and hydrogen. Then on time scales short compared to the diffusion time along field lines from the inside to the outside of the plasma ring, we may assume

$$n_I \sim n_e .$$

Furthermore, we assume constant electron pressure ($T_i \approx T_e$) on magnetic field lines, so that n_e changes locally according to $n_e \sim T_e^{-1}$. All assumptions result in a dependence of p_r on the local temperature on a field line according to

$$p_r \sim T_e^{\nu-2} .$$

Below a certain electron temperature (depending weakly on the impurity concentration) the typicl heat conduction time along field lines from outside to inside is longer than the local cooling time via radiation. The plasma is then unstable against a poloidal variation of the electron temperature if $\nu < 2$ in this range. For oxygen this will be the case for T_e above a few electron volts, depending slightly on the radiation model. Particle and heat transport across the unstable layer tend to stabilize this mode. Since the radial transport and especially its poloidal variation is not yet understood, a realistic modelling of the instability and its nonlinear

phase is difficult. Especially the latter is important since obviously a new, stable, highly asymmetric equilibrium state is reached sustained for many global energy or particle confinement times.

This new equilibrium is possible only if the local particle transport is extremly low and if there are appropriate sources and sinks. Infact, there are indications /2/ that the perpendicular transport is much lower on the inside of the plasma ring, where the low temperature anomaly occurs experimentally. Also classical parallel heat and particle transport along field lines is strongly inhibited by collisions in and near this low temperature region. But even a weakly anomalous cross diffusion and diffusion plus thermal forces (directed to high temperature at low impurity concentration /3/) along the magnetic field would restrict the local confinement of the cold plasma ring to less than 100 ms compared to 600 ms in the experiment.

With respect to sources we can probably rule out external impurity sources as pointed out above. For high n_e and low T_e, however, local recombination together with an appropriate mass flow could explain the experimentally observed spectral line intensities from low ionization states. A flow pattern similar to that in Pfirsch-Schlüter diffusion would probably be adequate. Since the local impurity content might be quite substantial, collisions between impurities may become important. Thermal force effects along field lines might separate impurities in different charge states and radial drifts could be induced. A description of these processes is beyond that in neoclassical theory because of the extreme local gradients involved.

In summary, the poloidal asymmetry is most probably the result of a thermal instability in the low temperature edge. The mechanisms involved in the highly asymmetric nonlinear state are not yet understood but, on the other hand, could provide new information about transport in tokamaks. A better understanding should also allow to estimate under which conditions the cold plasma zone expands unstably in radial direction thereby triggering a disruptive instability.

REFERENCES

/1/ Pickrell, M.M., Massachusetts Institute of Technology, Rep. PFC/RR-82-30

/2/ Keilhacker, M., Max-Planck-Institut für Plasmaphysik, Report IPP III/72, p. 1 (1981) and Physica Scripta T2, 443 (1982)

/3/ Neuhauser, J. et al., 11th Europ. Conf. on Contr. Fus. and Plasma Phys., Aachen, Sept. 1983, Contrib. Papers, Part II, p. 475

FIGURE CAPTIONS

Fig. 1: Density program, voltage of the fast gas valve and electron line density
a) in a discharge running into disruptions at the density limit
b) in a discharge staying stable in a predisruptive state.

Fig. 2: Neutral gas pressure, electron density and radiation in a discharge ended by disruptions at the density limit.

Fig. 3: Same parameters as in Fig. 2 for a discharge which stays stable in a predisruptive state.

Fig. 4: Time evolution of the line densities integrated along horizontal and vertical chords, resp., during the predisruptive state
a) in a divertor discharge
b) in a limiter discharge.

Fig. 5: Time evolution of the density profile at the plasma edge during the predisruptive state measured by means of a lithium probing beam.

Fig. 6: Density fluctuations observed by the HCN-interferometer.

Fig. 7: Correlation between the fluctuations on the HCN-interferometer signals and the fluctuations of the soft X-ray emission.

Fig. 8: Spatial distribution of the emission of hydrogen and impurity lines:
a) H_{β} before the predisruptive state
b) H_{β} during the predisruptive state
c) OII before the predisruptive state
d) OII during the predisruptive state
e) CII during the predisruptive state
f) CrI during the predisruptive state.
The photographs were taken through narrow band interference filters.

Fig. 9: Line integrated radial profiles of different oxygen lines. The profiles were scanned in vertical direction.

Fig. 10: Line integrated radial profiles of different carbon lines and OVI line. The profiles were scanned in vertical direction.

Fig. 11: Time evolution of the line emission from different ionization states of oxygen at the transition to the predisruptive state.

Fig. 12: Radial profiles of the total radiation measured by the bolometer.

Fig. 1

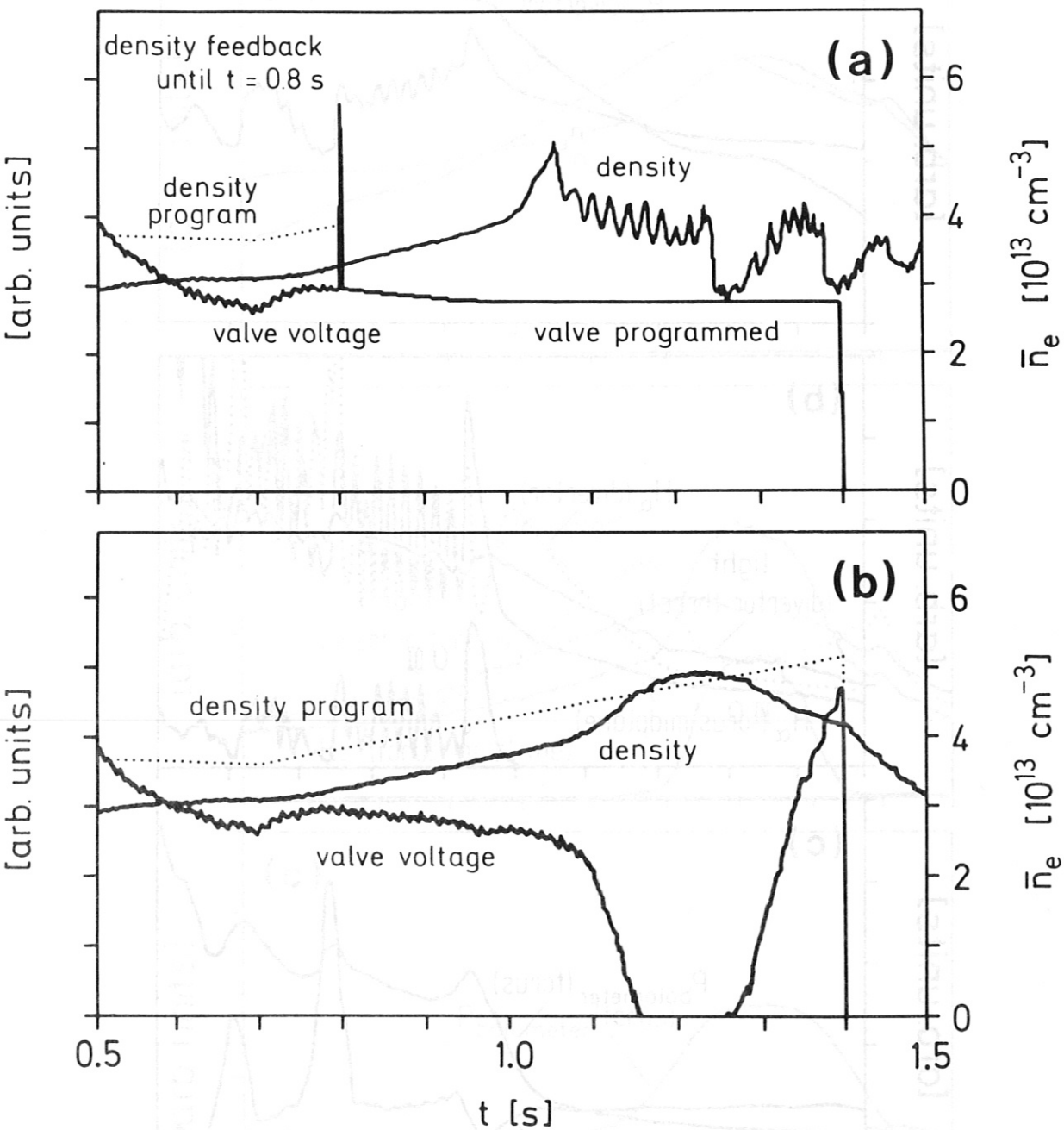
density feedback
until t = 0.8 s
(a)
density
density
program
valve voltage
valve programmed
[arb. units]
$\bar{n}_e$ [10^{13} cm^{-3}]
0
2
4
6
(b)
density program
density
valve voltage
[arb. units]
$\bar{n}_e$ [10^{13} cm^{-3}]
0
2
4
6
0.5
1.0
1.5
t [s]

Fig. 2

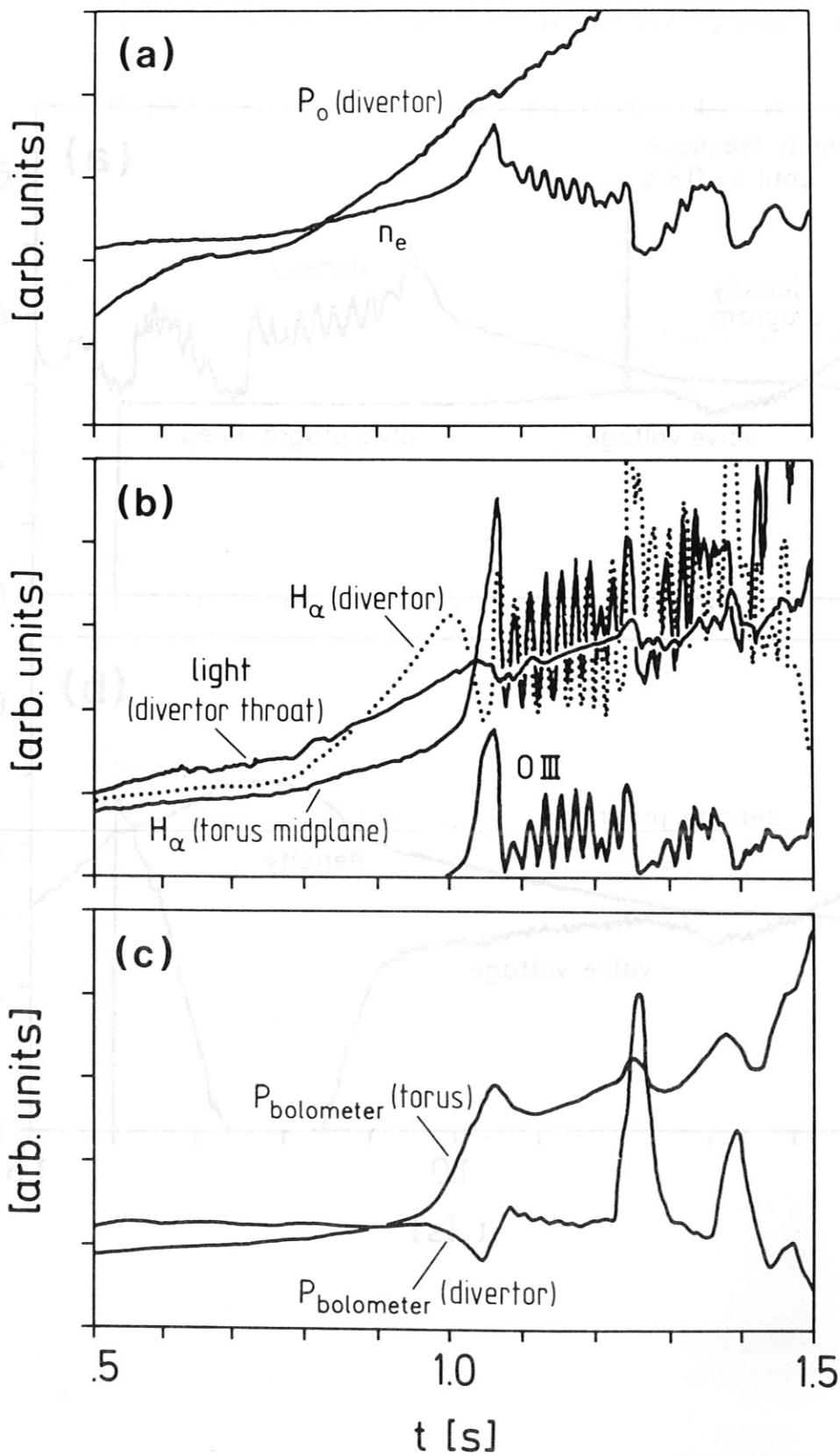
(a)
P_o (divertor)
n_e
[arb. units]
(b)
H_α (divertor)
light
(divertor throat)
O III
H_α (torus midplane)
[arb. units]
(c)
$P_{bolometer}$ (torus)
$P_{bolometer}$ (divertor)
[arb. units]
.5
1.0
1.5
t [s]

Fig. 3

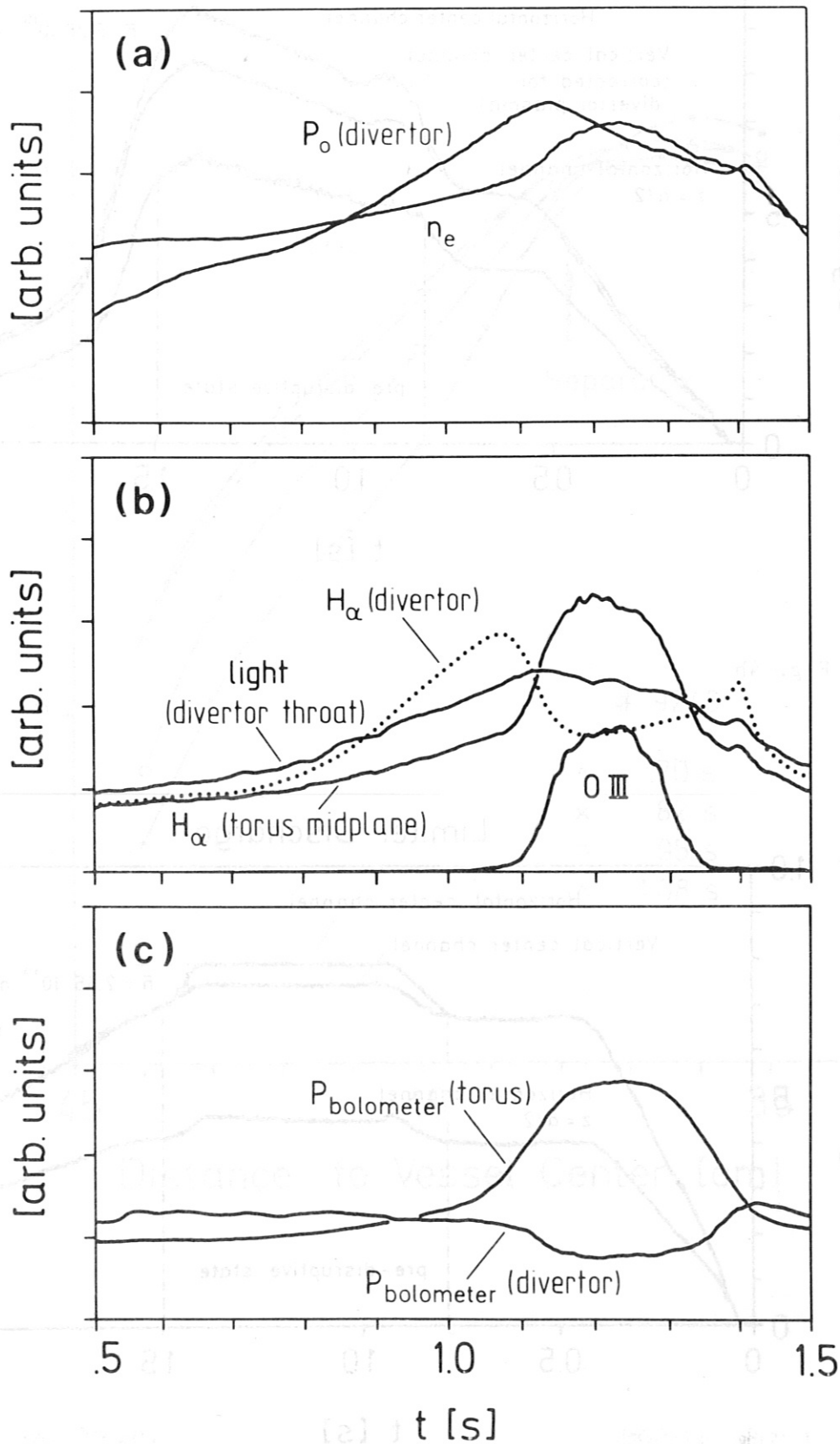
(a)
[arb. units]
P_o (divertor)
n_e
(b)
[arb. units]
H_α (divertor)
light
(divertor throat)
O III
H_α (torus midplane)
(c)
[arb. units]
$P_{bolometer}$ (torus)
$P_{bolometer}$ (divertor)
.5
1.0
1.5
t [s]

Fig. 4a

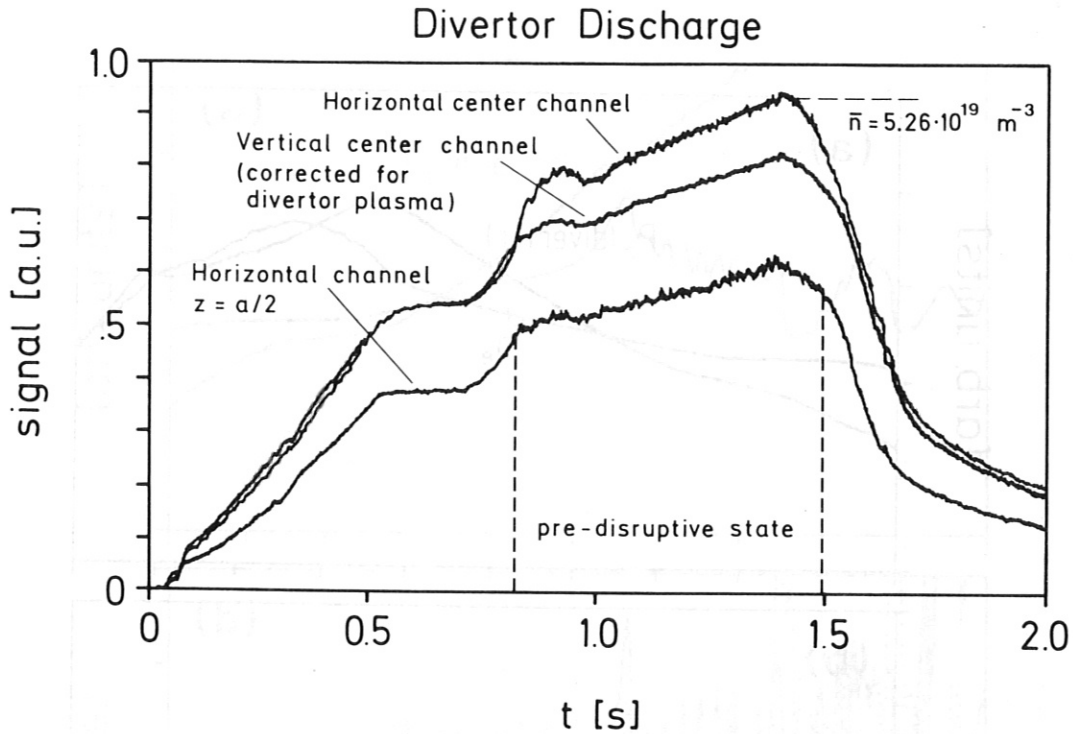
Divertor Discharge
1.0
.5
0
signal [a.u.]
Horizontal center channel
Vertical center channel
(corrected for
divertor plasma)
Horizontal channel
z = a/2
$\bar{n} = 5.26 \cdot 10^{19}$ m^{-3}
pre-disruptive state
0
0.5
1.0
1.5
2.0
t [s]

Fig. 4b

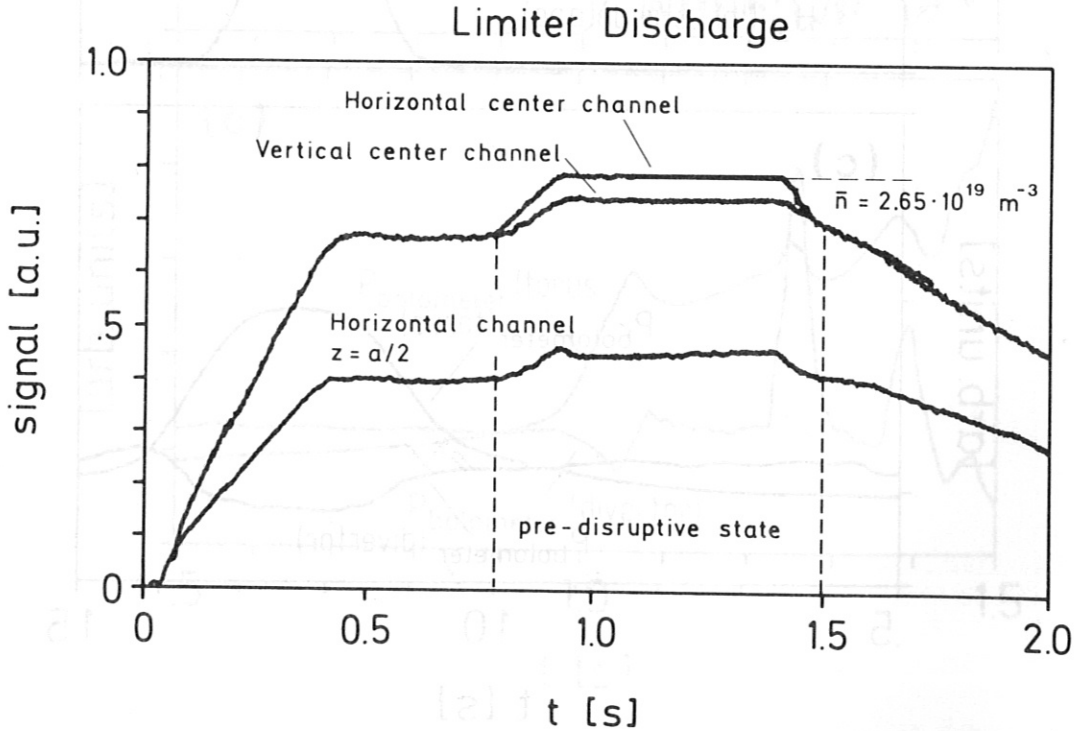
Limiter Discharge
1.0
.5
0
signal [a.u.]
Horizontal center channel
Vertical center channel
$\bar{n} = 2.65 \cdot 10^{19}$ m^{-3}
Horizontal channel
z = a/2
pre-disruptive state
0
0.5
1.0
1.5
2.0
t [s]

Fig. 5

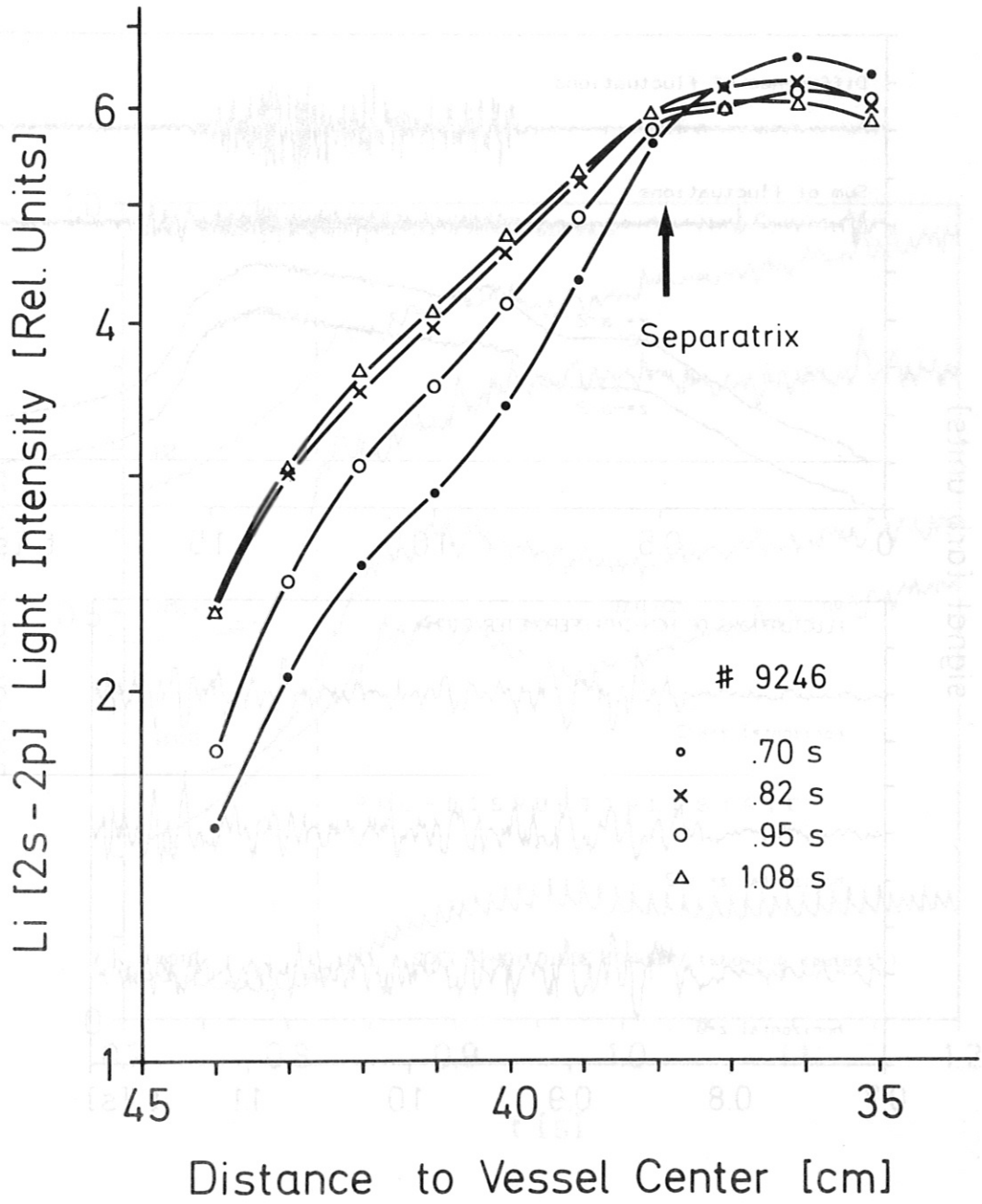
Li [2s - 2p] Light Intensity [Rel. Units]
6
4
2
1
45
40
35
Distance to Vessel Center [cm]
Separatrix
9246
.70 s
.82 s
.95 s
1.08 s

Fig. 6

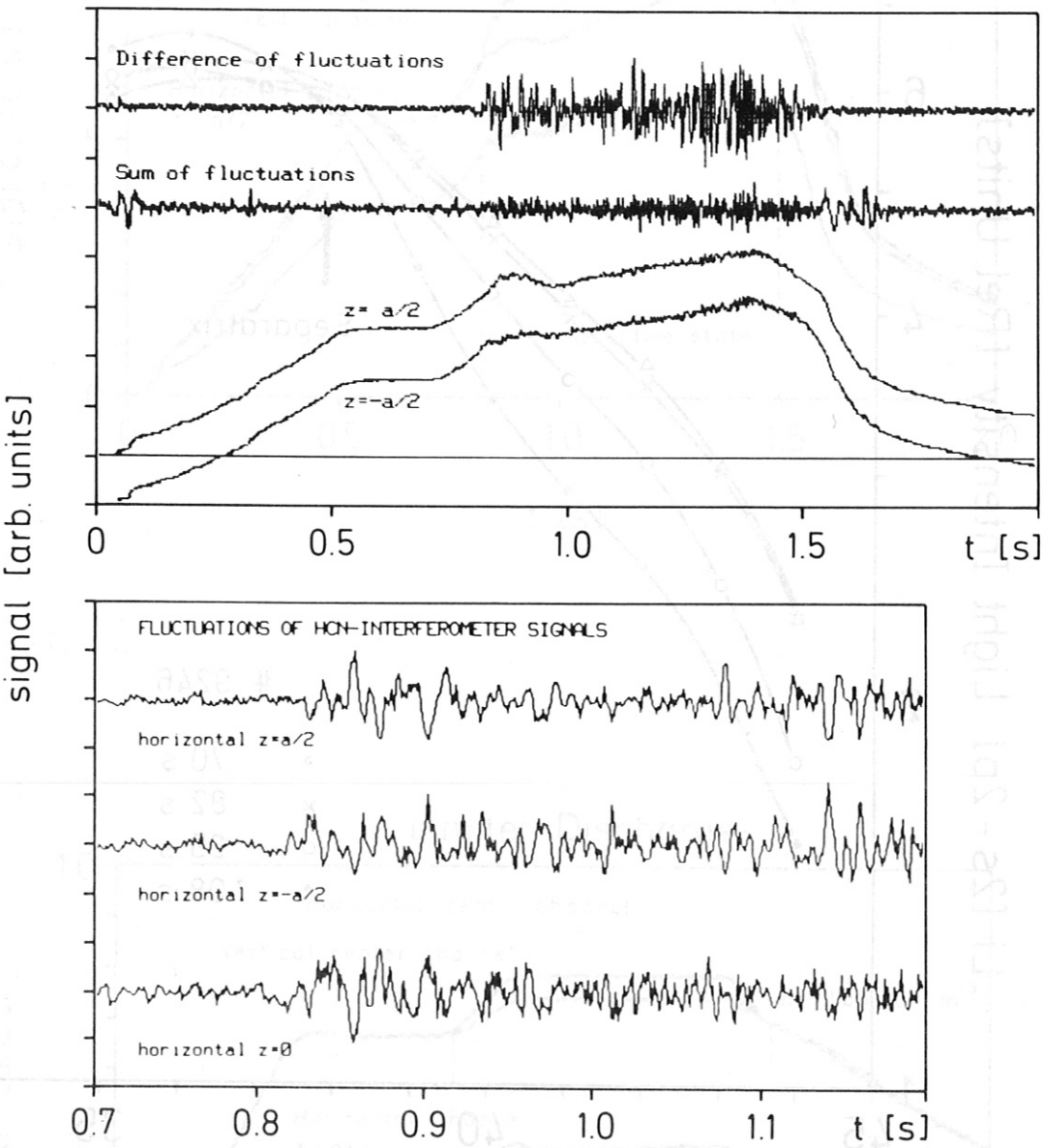
Difference of fluctuations
Sum of fluctuations
z= a/2
z=-a/2
0
0.5
1.0
1.5
t [s]
signal [arb. units]
FLUCTUATIONS OF HCN-INTERFEROMETER SIGNALS
horizontal z=a/2
horizontal z=-a/2
horizontal z=0
0.7
0.8
0.9
1.0
1.1
t [s]

Fig. 7

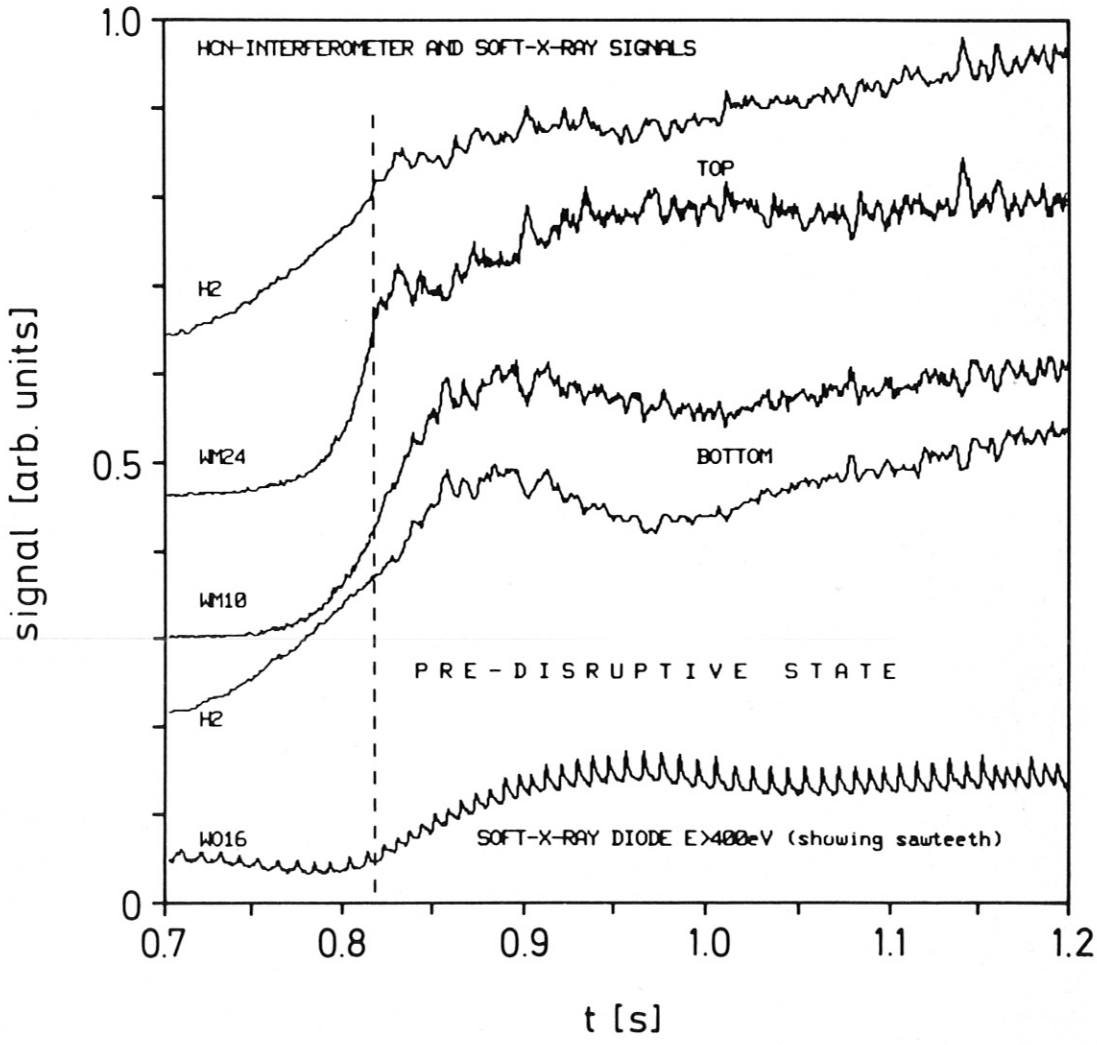
HCN-INTERFEROMETER AND SOFT-X-RAY SIGNALS
TOP
H2
WM24
BOTTOM
WM10
PRE-DISRUPTIVE STATE
H2
WO16
SOFT-X-RAY DIODE E>400eV (showing sawteeth)
signal [arb. units]
t [s]
1.0
0.5
0
0.7
0.8
0.9
1.0
1.1
1.2

Fig. 8a

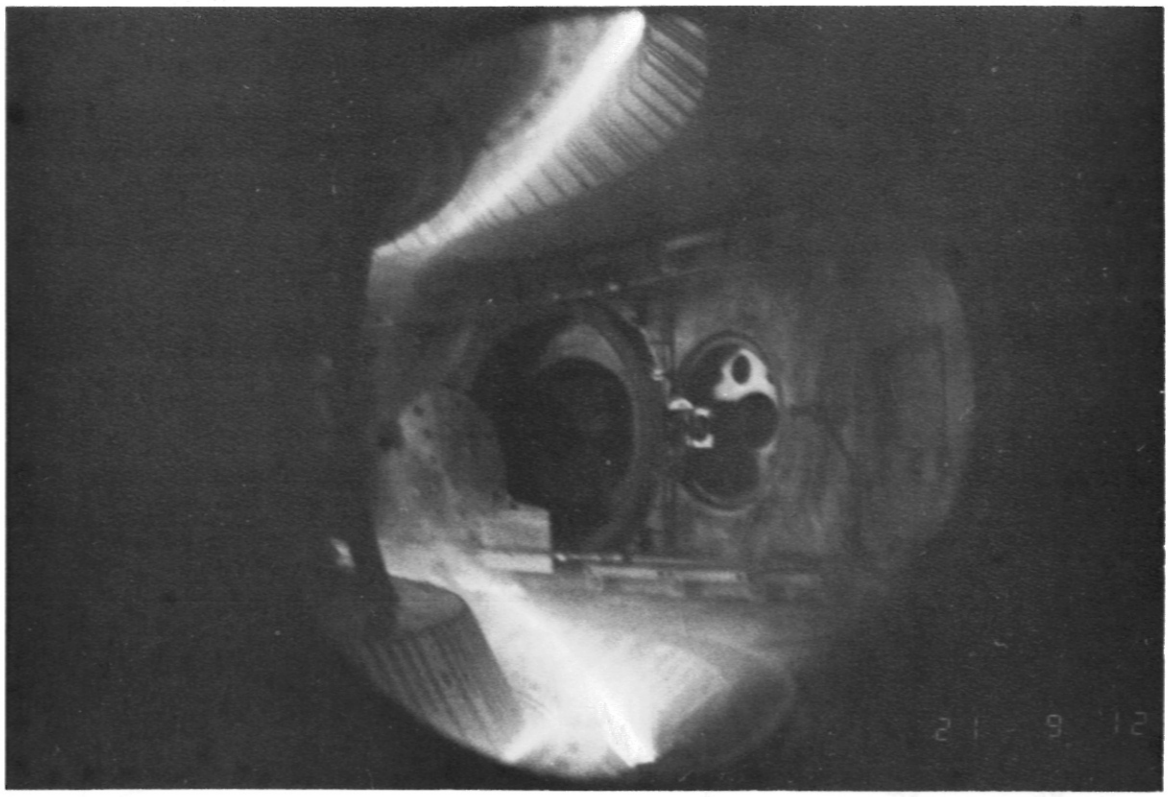

Fig. 8b

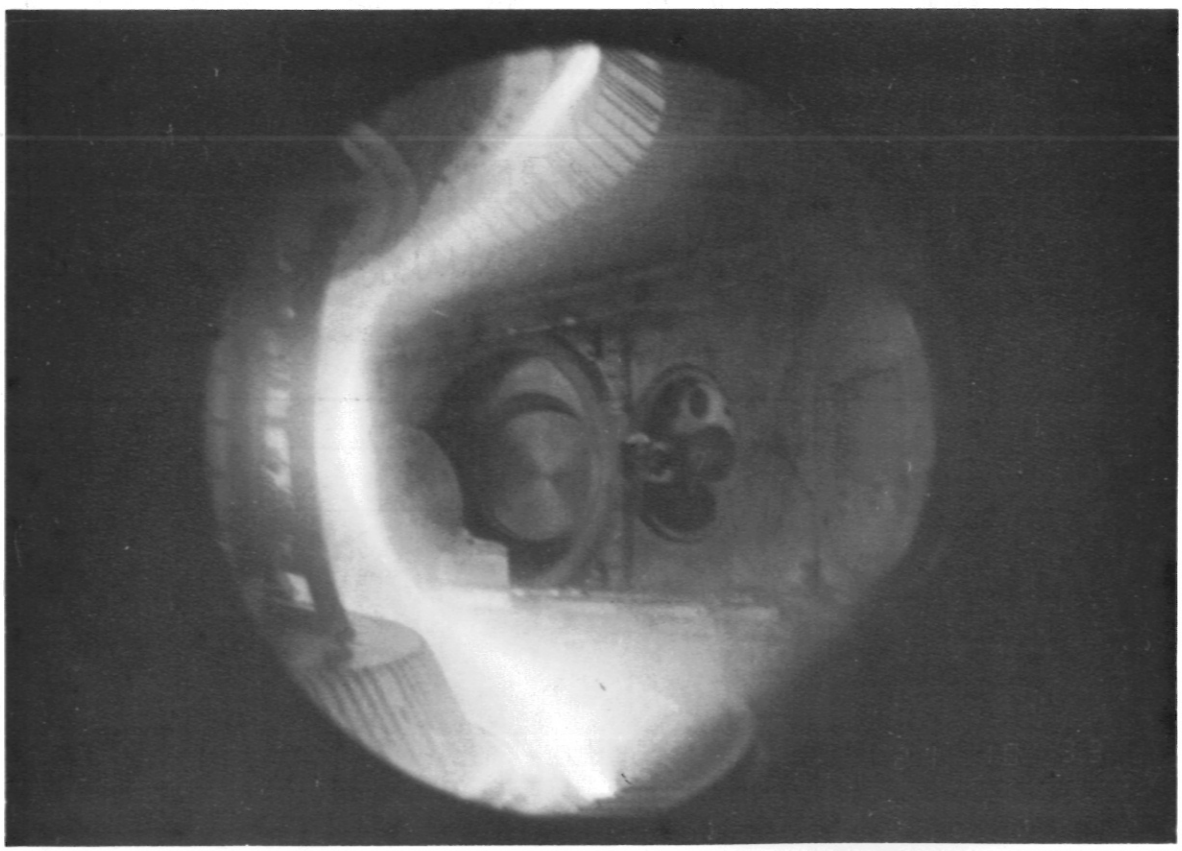

Fig. 8c

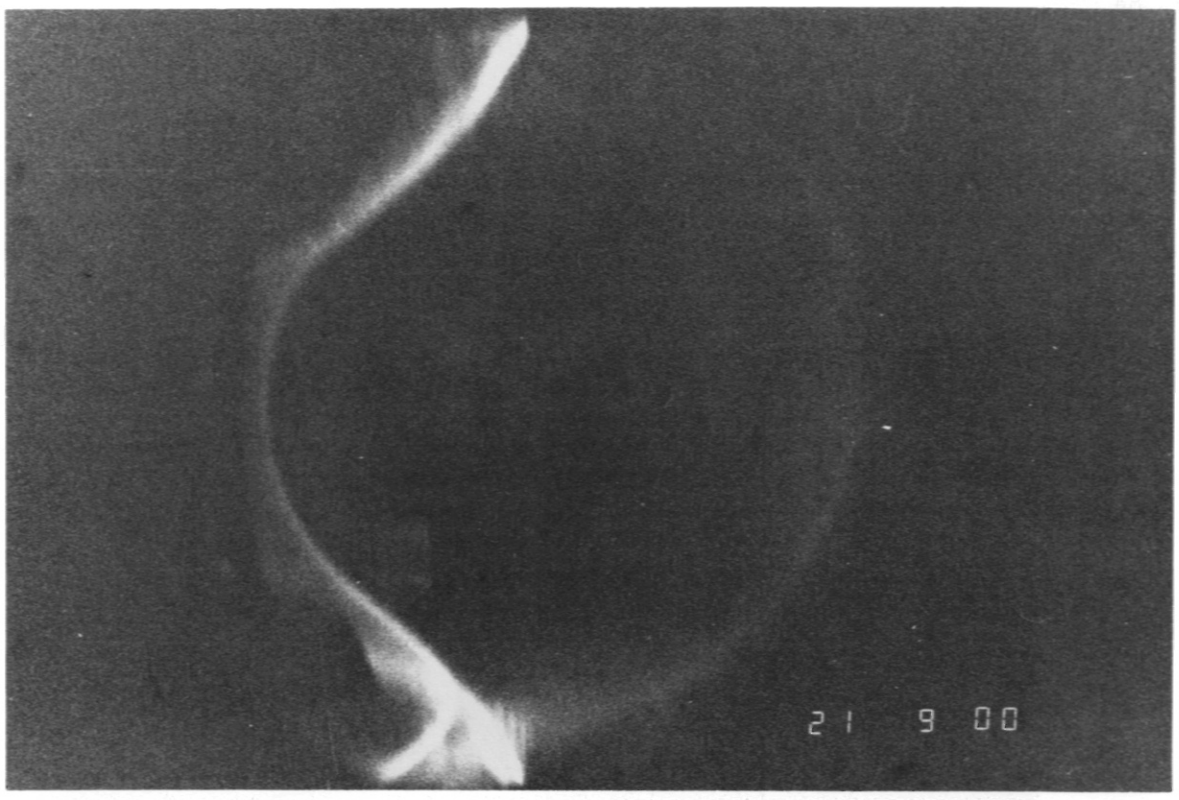

Fig. 8d

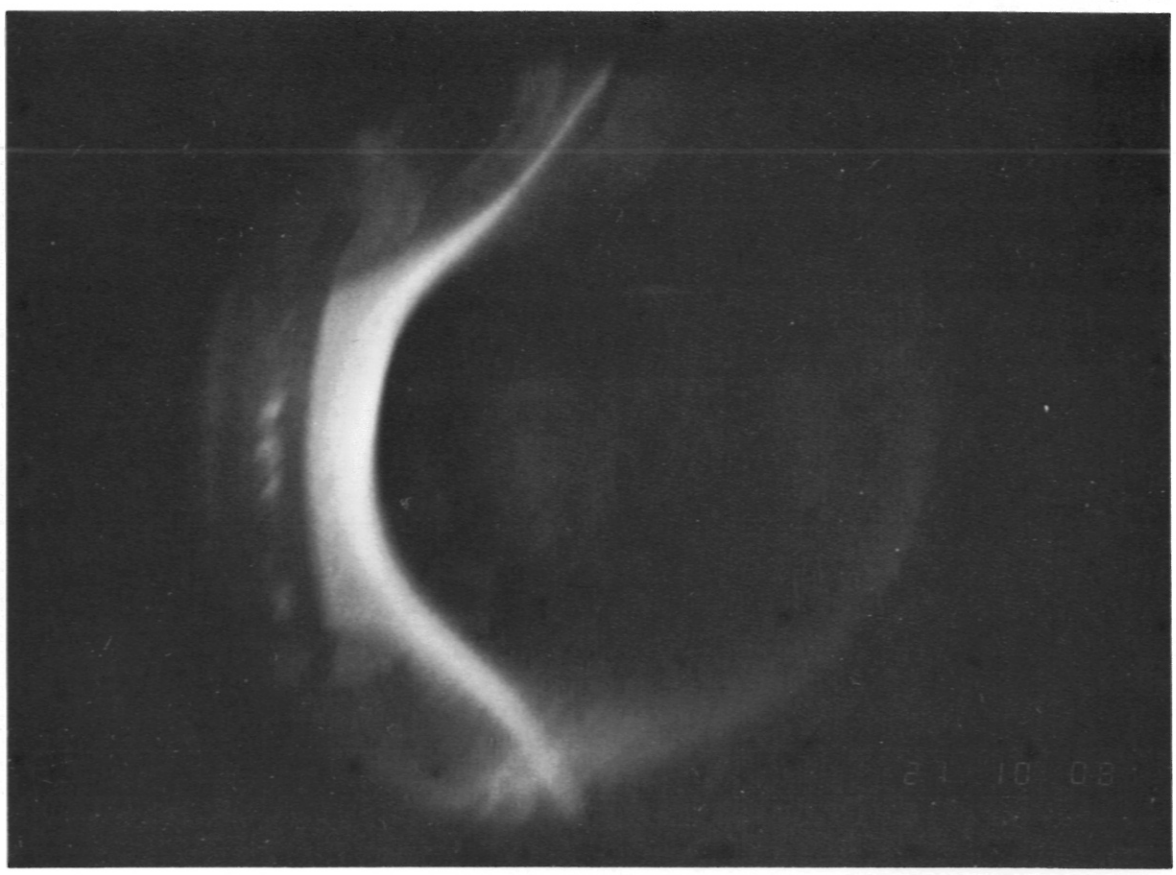

Fig. 8e

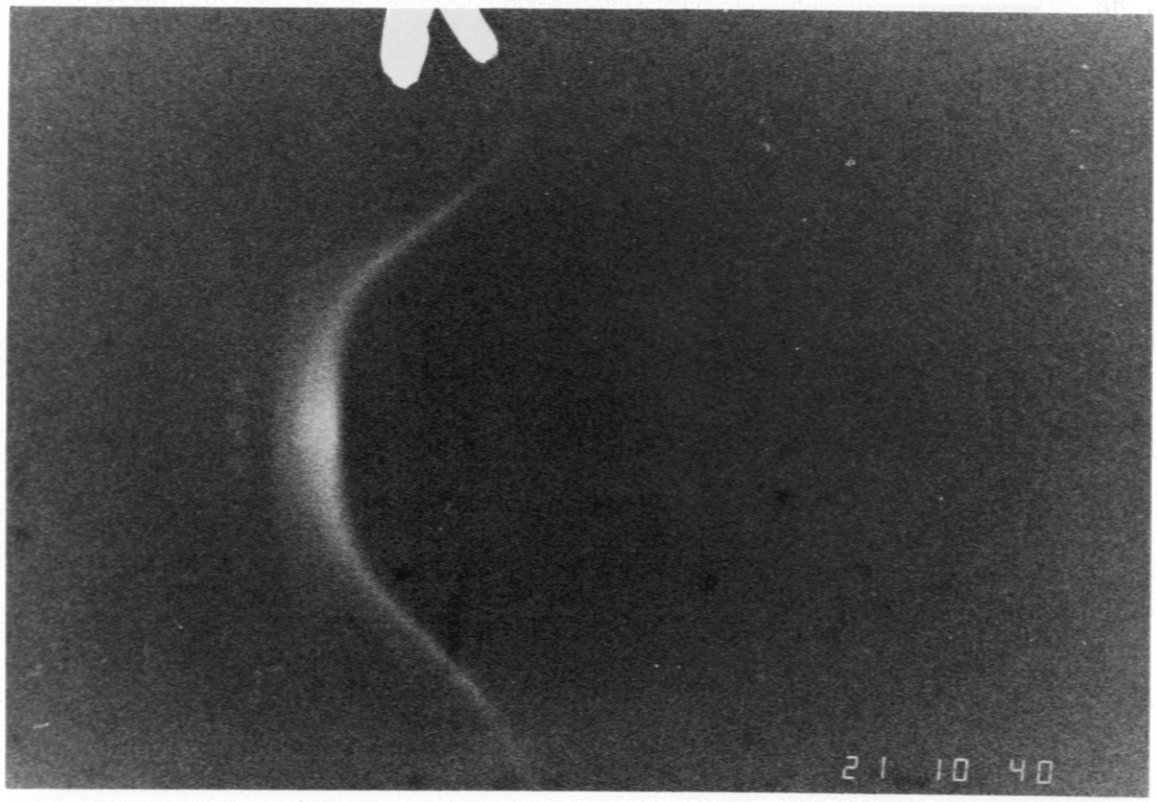

Fig. 8f

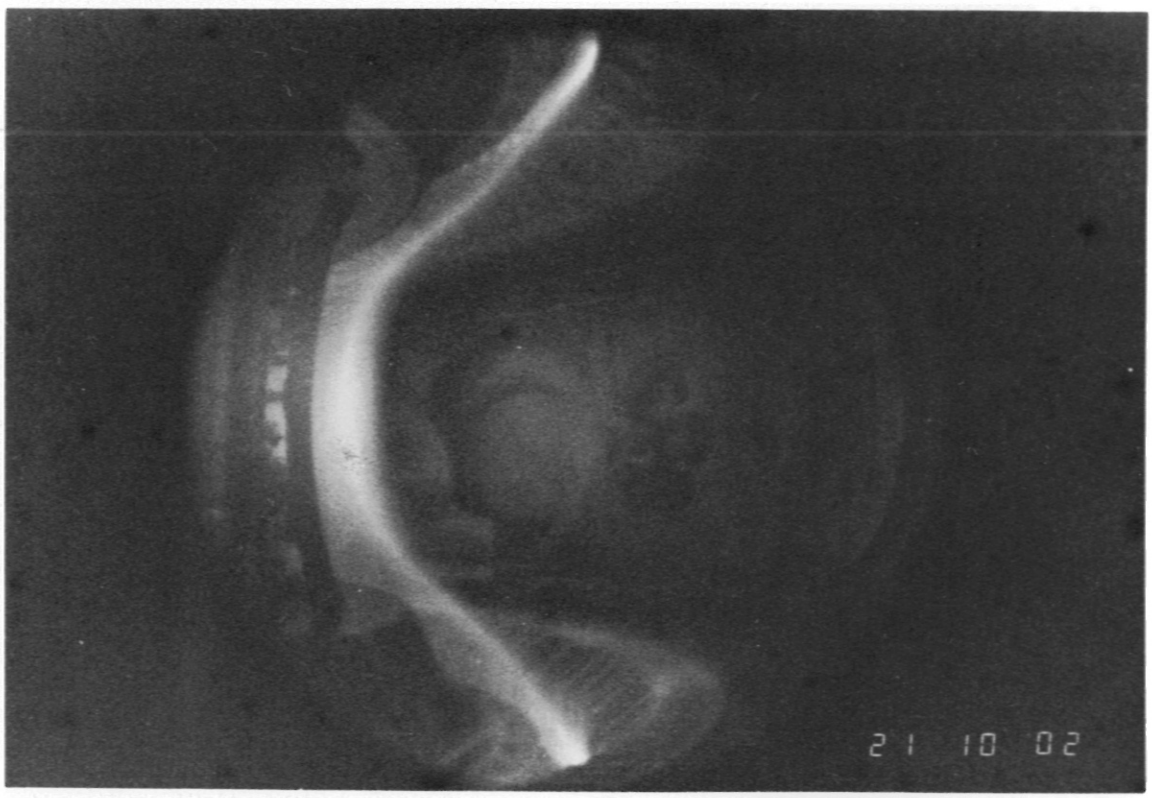

Fig. 9

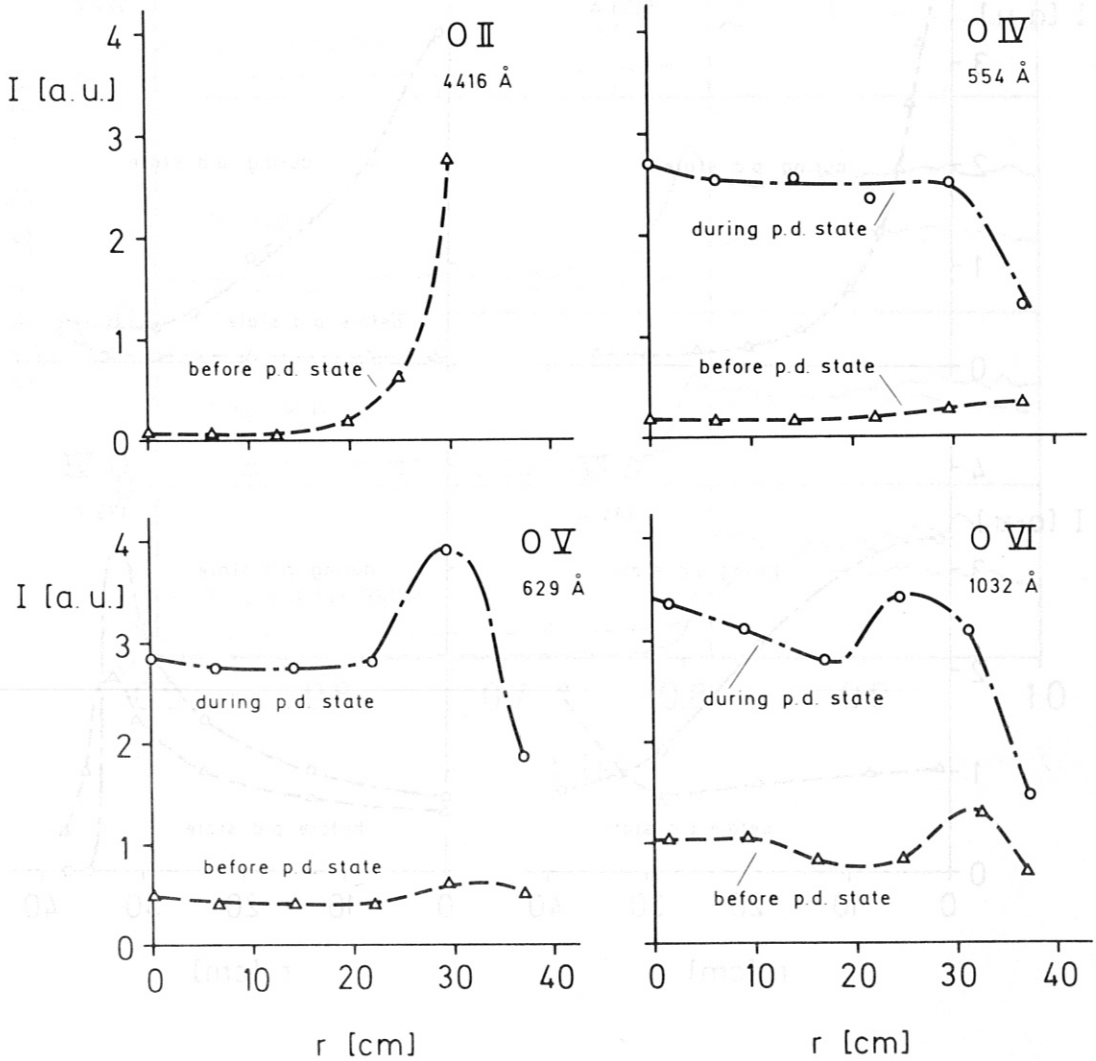
O II
4416 Å
O IV
554 Å
O V
629 Å
O VI
1032 Å
I [a.u.]
I [a.u.]
during p.d. state
before p.d. state
during p.d. state
before p.d. state
during p.d. state
before p.d. state
during p.d. state
before p.d. state
0
1
2
3
4
0
10
20
30
40
r [cm]
r [cm]

Fig. 10

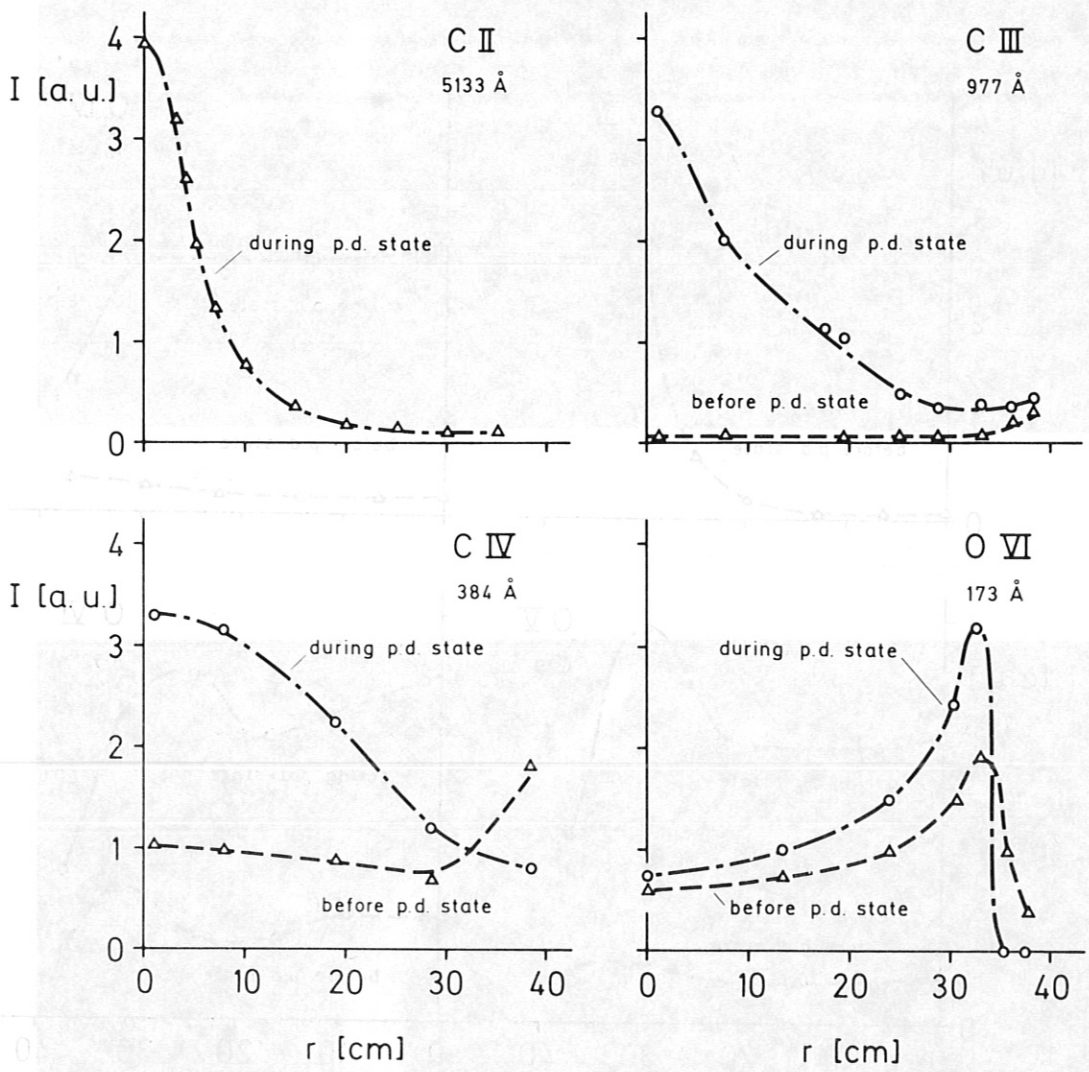
C II
5133 Å
during p.d. state
C III
977 Å
during p.d. state
before p.d. state
C IV
384 Å
during p.d. state
before p.d. state
O VI
173 Å
during p.d. state
before p.d. state
I [a.u.]
I [a.u.]
0
1
2
3
4
0
10
20
30
40
r [cm]
r [cm]

Fig. 11

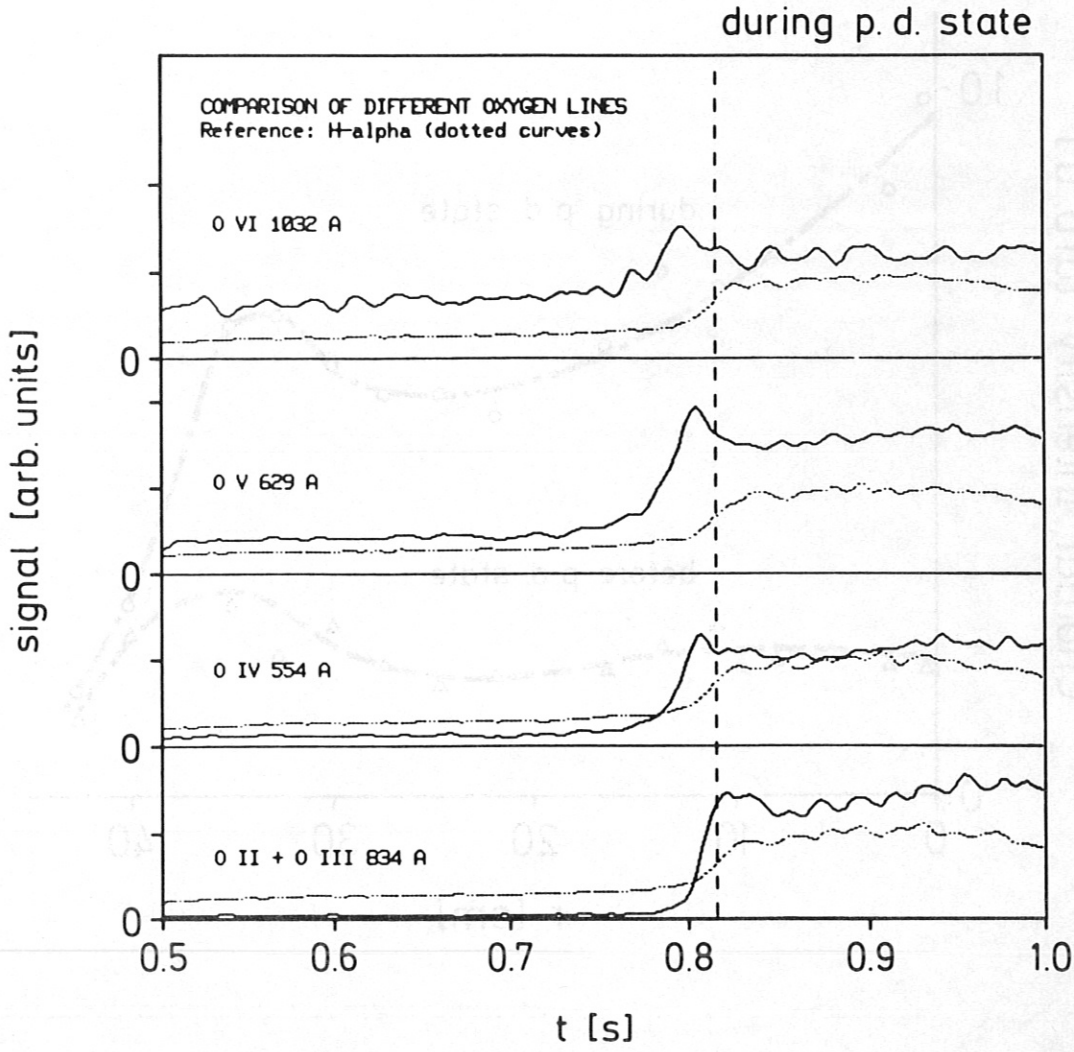
during p. d. state
COMPARISON OF DIFFERENT OXYGEN LINES
Reference: H-alpha (dotted curves)
O VI 1032 A
O V 629 A
O IV 554 A
O II + O III 834 A
signal [arb. units]
0
0
0
0
0.5
0.6
0.7
0.8
0.9
1.0
t [s]

Fig. 12

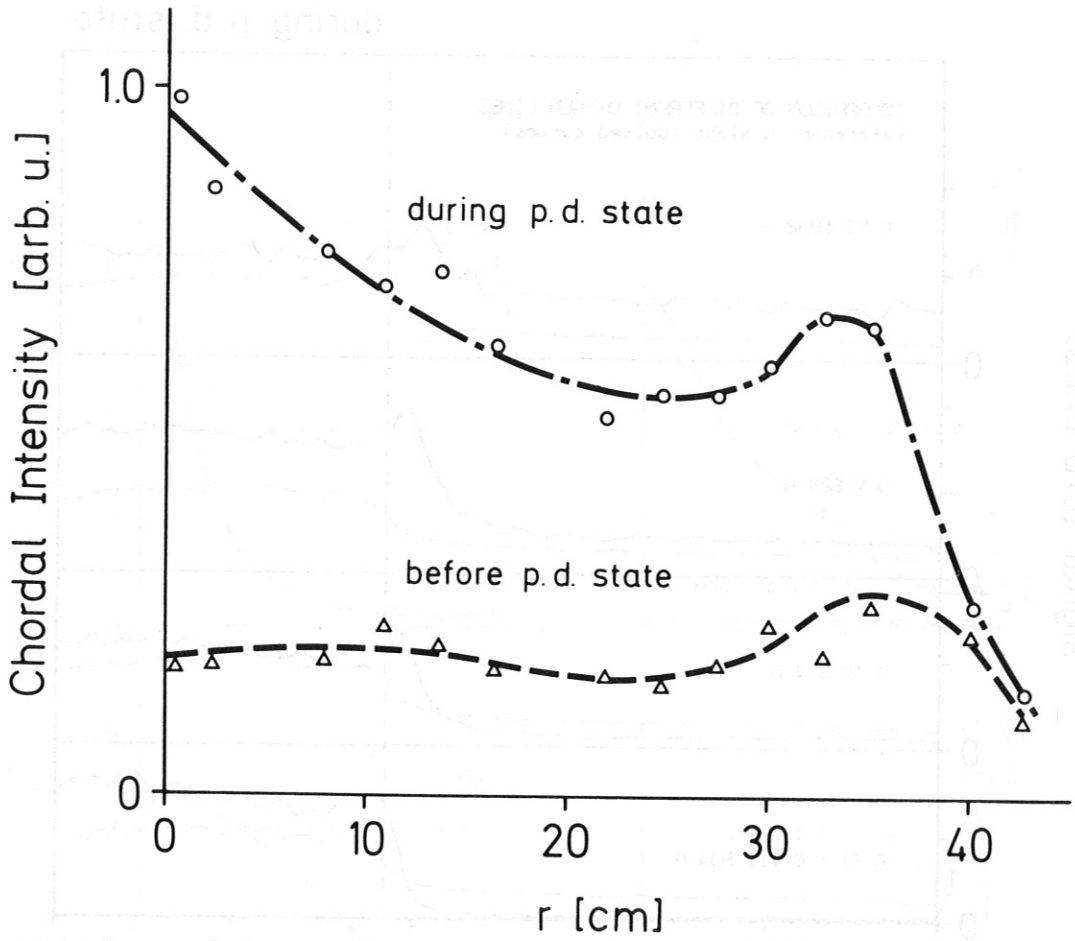
Chordal Intensity [arb. u.]
1.0
0
during p.d. state
before p.d. state
0
10
20
30
40
r [cm]